Appl. Phys. B 84, 205–210 (2006)
DOI: 10.1007/s00340-006-2229-7

Applied Physics B
Lasers and Optics

D.A. GENOV[1]
K. SEAL[2,✉]
A.K. SARYCHEV[3]
H. NOH[2]
V.M. SHALAEV[4]
Z.C. YING[5]
X. ZHANG[1]
H. CAO[2]

Surface plasmon delocalization by short-range correlations in percolating metal systems

[1] NSF Nanoscale Science and Engineering Center, University of California, Berkeley, CA 94720, USA
[2] Department of Physics and Astronomy, Northwestern University, Evanston, IL 60208, USA
[3] Ethertronics Inc., 9605 Scranton Road, Suite 850, San Diego, CA 92121, USA
[4] School of Electrical and Computer Engineering, Purdue University, West Lafayette, IN 47907, USA
[5] National Institute of Standards and Technology, Gaithersburg, MD 20899, USA

Received: 1 February 2006
Published online: 5 May 2006 •

ABSTRACT Theoretical and experimental studies of the electromagnetic response of semicontinuous metal films are presented. A scaling theory is developed by solving the surface plasmon eigenproblem. The short-range correlations in the governing Kirchhoff Hamiltonian result in delocalization of the surface plasmon eigenmodes. Although their relative weight in the spectrum becomes asymptotically small for large systems, the existence of these delocalized states modifies the critical indices for the high-order field moments. This modification is confirmed experimentally by the near-field measurement of high-order intensity moments for percolating silver films on glass substrates.

PACS 68.37.Uv; 73.20.Mf; 42.25.Dd; 78.67.-n

1 Introduction

Metal–dielectric nanocomposites have attracted a large amount of interest in recent years due to their exceptional optical properties. Resonant excitation of surface plasmons (SPs) enables concentration and transfer of electromagnetic energy over nanoscaled regions, making these composite systems very different from their constituent materials [1–20]. Several studies have focused on the field distribution on the surface of random 2-D metal–dielectric systems such as semicontinuous metal films near the percolation threshold [1–3, 6–9, 16–18, 20]. It has been theoretically predicted [1–11] and experimentally confirmed [12–20] that when light is made incident on these samples, electromagnetic energy can be localized in subwavelength areas. These 'hot spots', which may be as small as a few nanometers, can exhibit giant local field enhancement. As a result, the field distribution on the surface of these structures is extremely inhomogeneous [2–5, 8].

Theoretical modeling of SPs in planar random metallic nanostructures initially involved the use of a Hamiltonian similar to the Anderson Hamiltonian of an electronic system [21]. The uncorrelated random potential in the Anderson model results in exponential localization of the electronic wave functions in 1-D and 2-D systems [21–23]. The spatial localization of the electron wave function implies that each electron is bound in a particular region of space, and thus electron transport through the random system is impeded. Due to similarity with the Anderson model, it was believed that the SP modes of random metallic systems were localized as well [1, 2, 8]. However, recent theoretical studies of random planar metal–dielectric composites have shown that the SP modes of such systems are not strongly (Anderson) localized and there is a significant presence of delocalized modes [3]. The coexistence of localized modes and delocalized modes [3, 6] makes it difficult to experimentally probe the delocalized states.

In this paper we demonstrate that short-range correlations in the governing Kirchhoff Hamiltonian (KH) result in delocalization of the SP eigenmodes in semicontinuous metal films at the percolation threshold. The subset of these modes has a zero measure, so that their relative weight in the spectrum becomes asymptotically small for large systems. This study aims at finding the manifestation of these delocalized modes from the optical response of the composite. We find theoretically that the singularity caused by the delocalized states results in modification of the critical indices for the high-order field moments. This modification is probed experimentally for percolating silver films by near-field scanning optical microscopy. By comparing the measured local field moments to the numerically calculated values, we extract the degree of delocalization and prove the existence of delocalized SP states.

2 Theory and numerical calculations

Random metal–dielectric composites comprise nanosized metal particles on a dielectric substrate. In the visible and infrared spectral ranges, the metal conductivity σ_m is a complex number with a positive imaginary part σ_m'' and a small real part σ_m' (representing losses in metal). Therefore, a metal particle can be viewed as an inductance L connected in series with a resistance R, while the dielectric host is modeled as a capacitance C. Relying on this model, one may think of the inhomogeneous metal film as a random network of RLC circuits [2, 24]. The geometrical disorder in such systems leads to a broad range of SP resonances (corresponding

✉ Fax: 847 491 9982, E-mail: k-seal@northwestern.edu

to equivalent *RLC* resonances) and strong enhancement of the local electric fields [2, 16].

To investigate the SP modes that are excited on the film surfaces, we restrict our study to composites of metal particles with sizes much smaller than the wavelength of illumination, $a \ll \lambda$. Under this condition one can neglect retardation effects and seek a solution for the local potential in the quasi-static approximation. The resulting 'generalized' current conservation has the form

$$\nabla \cdot [\sigma(\boldsymbol{r})(-\nabla\varphi(\boldsymbol{r}) + \boldsymbol{E}_0)] = 0\,, \tag{1}$$

where $\sigma(\boldsymbol{r})$ is the spatially dependent local conductivity, $\varphi(\boldsymbol{r})$ describes the local potential and $\boldsymbol{E}_0$ is the external field. In our model we assign to $\sigma(\boldsymbol{r})$ a metal conductivity σ_m with probability p or a dielectric conductivity σ_d with probability $1-p$. Discretization of (1) on a square lattice with size L leads to a system of L^2 linear equations $\hat{\boldsymbol{H}} \cdot \boldsymbol{\Phi} = \boldsymbol{F}$, where the matrix $\hat{\boldsymbol{H}}$ is the Kirchhoff Hamiltonian (KH), while the vectors $\boldsymbol{\Phi}$ and $\boldsymbol{F}$ are the local potentials and externally induced currents, respectively. The KH is a symmetric random matrix with diagonal elements given by the sum $H_{ii} = \sum_j \sigma_{ij}$ of all bond conductivities σ_{ij} that connect the ith site with its nearest neighbors and off-diagonal elements $H_{ij} = -\sigma_{ij}$. Due to the random nature of the conductivities σ_{ij} the KH is thus mathematically similar to the Anderson Hamiltonian (AH) that is studied in quantum mechanics [1, 22]. However, unlike the AH, the diagonal and off-diagonal elements of the KH are not independent. The correlations are due to the local current conservation, and as we will show later they result in dramatic changes in the nature of the SP localization as compared to the discrete non-correlated Anderson analogue.

In order to simplify the treatment of the SP excitation in metal–dielectric films, we first work in the regime of single-particle resonance, $\varepsilon'_\mathrm{m} = -\varepsilon_\mathrm{d}$, where the dielectric constants $\varepsilon_s = 4\pi \mathrm{i}\sigma_s/\omega_\mathrm{r}$ depend on the complex conductivities σ_s (s stands for the metal or the dielectric components) and the resonance frequency ω_r. Next, we normalize (1) by σ_d and use a new set of non-dimensional permittivities $\varepsilon^*_\mathrm{d} = 1$ and $\varepsilon^*_\mathrm{m} = -1 + \mathrm{i}\kappa$, where for noble metals and visible light the losses are small: $\kappa = \varepsilon''_\mathrm{m}/|\varepsilon'_\mathrm{m}| \ll 1$. Following the scaling theory [1], we seek a general solution of (1) as an expansion over the eigenstates Ψ_n of the SP eigenproblem

$$\nabla \cdot [\theta(\boldsymbol{r})\nabla\Psi_n(\boldsymbol{r})] = \Lambda_n \Psi_n(\boldsymbol{r})\,, \tag{2}$$

where the topology function $\theta(\boldsymbol{r}) = \pm 1$ maps the real part of the non-dimensional dielectric constant $\varepsilon^*(\boldsymbol{r})$ and thus corresponds only to geometrical characteristics of the film. Specifically, the reduction of (3) on a square lattice results in a matrix equation $\hat{\boldsymbol{H}}' \cdot \boldsymbol{\Psi}_n = \Lambda_n \boldsymbol{\Psi}_n$, where $\hat{\boldsymbol{H}}'$ is the real part of the normalized KH and has the same correlation properties. These correlations can also be represented through the covariance matrices $\hat{\boldsymbol{G}}^{\mathrm{d-d}}$ and $\hat{\boldsymbol{G}}^{\mathrm{d-o}}$ that describe the statistical dependences between the diagonal $\{d_i\}$ and off-diagonal $\{o_i\}$ elements of the matrix $\hat{\boldsymbol{H}}'$. Specifically, for the diagonal elements we have $G^{\mathrm{d-d}}_{ij} = E[(d_i - \overline{d})(d_j - \overline{d})] = \sigma^2_\mathrm{o}(\delta_{i,j\pm1} + \delta_{i,j\pm L} + 4\delta_{ij})$, where E is the expectation value and σ_o is the standard deviation of the off-diagonal elements. For the correlations between diagonal and off-diagonal elements we have $G^{\mathrm{d-o}}_{ij} = E[(d_i - \overline{d})(o_j - \overline{o})] = \sigma^2_\mathrm{o}(\delta_{i,j-1} + \delta_{ij})$, where we have taken into consideration the first to the right off-diagonal vector, but similar relationships hold for the rest of the off-diagonal vectors. For all cases, at the percolation threshold $p = p_\mathrm{c}$ we have $\sigma_\mathrm{o} = 1$ and $\overline{d} = \overline{o} = 0$.

We solve the SP eigenproblem by using Neumann-type boundary conditions, thus assuring the conservation of the local currents at the film boundaries. For example, we use $\theta(\boldsymbol{r})[\boldsymbol{n} \cdot \nabla\Psi_n(\boldsymbol{r})]|_{x=0} = \theta(\boldsymbol{r})[\boldsymbol{n} \cdot \nabla\Psi_n(\boldsymbol{r})]|_{x=L}$ at the left and right sample boundaries. Alternatively, electrode-type boundary or 'natural' boundary conditions ($H'_{ii} = 1$, at the boundary) can be applied.

To begin our analysis of the SP eigenproblem we first examine some specific eigenmodes. For metal–dielectric films at the percolation threshold, we distinguish two limiting cases. In the first case presented in Fig. 1a, the SP eigenmode situated at the band edge is strongly localized. However, the nature of the eigenstates at the band center (see Fig. 1b) is

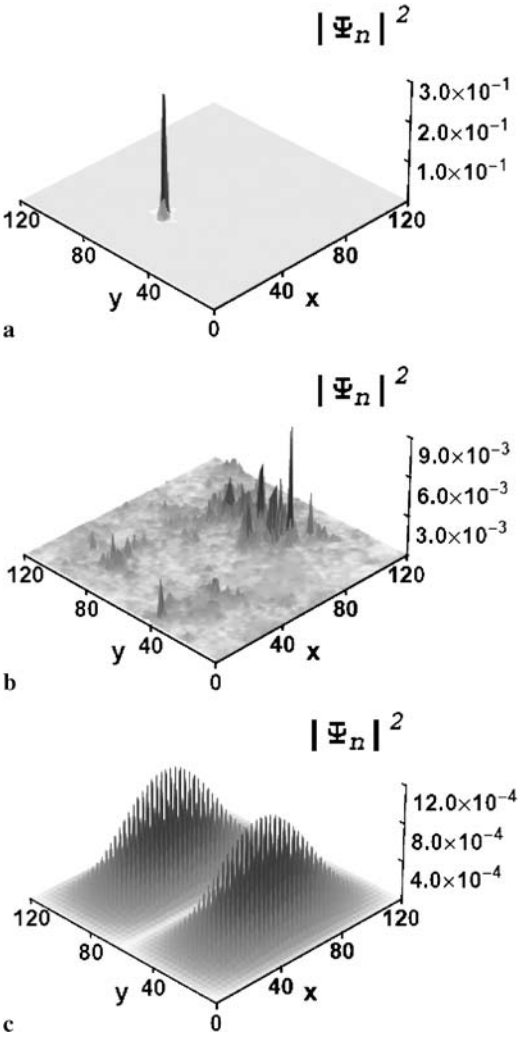

FIGURE 1 Surface plasmon eigenmodes in random (**a**), (**b**) and periodic (**c**) metal–dielectric films. The corresponding eigenvalues are (**a**) $\Lambda = -5.6945$ (localized), (**b**) $\Lambda = 0.0044$ (delocalized) and (**c**) $\Lambda = -5.9974$ (periodic)

completely different. Those states are extended and according to our studies (not presented here) they exhibit multifractal properties. In Fig. 1c we also show a particular SP mode that is manifested in the periodic case. The periodic structure is modeled as a square lattice of metal particles with metal coverage equal to 2/3. The important feature to be recognized here is the presence of two length scales, one corresponding to the macroscopically extended Bloch states and the second to local oscillations on the scale of a single particle. We believe that the microscopic SP eigenmode fluctuations correspond to a strong inhomogeneity of the electromagnetic fields observed even for a perfectly ordered metal–dielectric film [25].

The statistical properties of the SP eigenproblem are investigated in terms of the density of states $\varrho(\Lambda)$ and SP localization lengths $\xi(\Lambda)$. Both characteristics are studied for the KH and for the corresponding discrete, non-correlated AH. To simulate the AH we rely on the fact that for each metal concentration p the elements of the matrix $\hat{\boldsymbol{H}}'$ take discrete values with a specific probability. Those probability distributions are then used to build up the AH without enforcing correlations between its elements.

In Fig. 2a we show that both correlated and non-correlated eigenproblems have quite similar densities of states for most of the spectrum. However, at the band center we observe a singularity in the case of the KH. To better understand this important peculiarity, we plot (see the inset in Fig. 2a) the region of very small eigenvalues ($\Lambda \ll 1$) on a log–log scale.

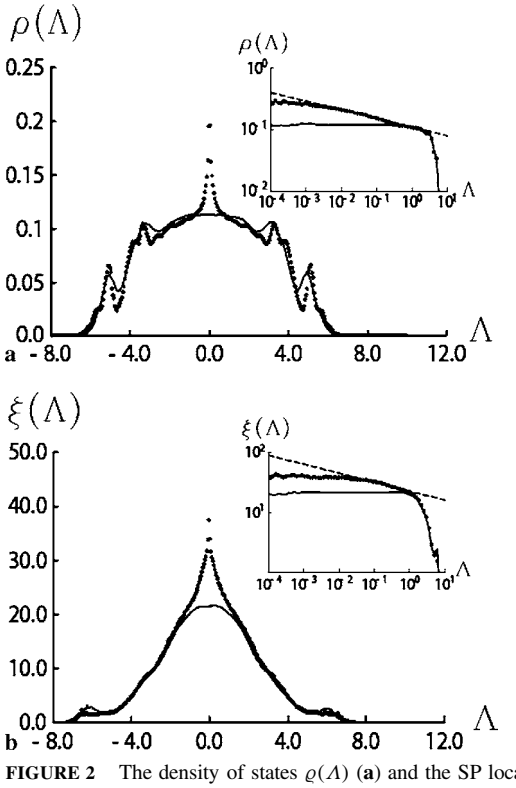

FIGURE 2 The density of states $\varrho(\Lambda)$ (**a**) and the SP localization lengths $\xi(\Lambda)$ (**b**) for the KH (*dots*) and for the corresponding Anderson problem (*solid line*), calculated at the resonant condition $\varepsilon_{\mathrm{d}}^{*} = -\varepsilon_{\mathrm{m}}^{*} = 1$. The band-center singularity is shown in the log–log *insets*, where a power-law fit (*dashed line*) with exponent $\gamma = \alpha = 0.14$ is applied. The data is averaged over 100 different realizations of percolation samples each with size $L = 120$

In the first approximation the density of states seems to diverge as a power law $\varrho(\Lambda) \simeq A|\Lambda|^{-\gamma}$, where A is a normalization constant and $\gamma = 0.14 \pm 0.01$ is a critical exponent. However, a logarithmic singularity $\varrho(\Lambda) \simeq A[1 + \ln(|\Lambda|^{-\gamma})]$ also fits the result. Those two functions are virtually identical in a broad range of the arguments $\mathrm{e}^{1/\gamma} \gg |\Lambda| \gg \mathrm{e}^{-1/\gamma}$, and therefore for simplicity in the scaling theory that follows we use the power-law relationship. In Fig. 2a we have also included the result for the non-correlated AH case, where the density of states is relatively uniform throughout the spectra and does not show any singularities, which matches our expectations.

The role of the cross correlations presented in the KH eigenproblem is next studied in terms of the SP localization lengths $\xi(\Lambda)$. The localization length for each eigenmode is calculated using the gyration radius $\xi^2(\Lambda_n) = \int (\boldsymbol{r} - \langle \boldsymbol{r} \rangle_n)^2 |\Psi_n(\boldsymbol{r})|^2 \,\mathrm{d}\boldsymbol{r}$, where $\langle \boldsymbol{r} \rangle_n = \int \boldsymbol{r} |\Psi_n(\boldsymbol{r})|^2 \,\mathrm{d}\boldsymbol{r}$ is the 'mass center' of the nth mode and the integration is performed over the film surface. The results for $\xi(\Lambda)$ are presented in Fig. 2b. Similar to what we have observed for the density of states (see Fig. 2a), there is a singularity at the band center for the KH. The localization length diverges logarithmically for $\Lambda \to 0$, but also can be fitted with a power law $\xi(\Lambda) \sim |\Lambda|^{-\alpha}$, where $\alpha = 0.15 \pm 0.02$. The size effect is clearly visible for the extended states with $\xi(\Lambda) \geq L$.

The existence of delocalized states has been recently predicted for a somewhat similar (but not the same) SP eigenproblem in [3], where it was concluded that those modes play a dominant role in the interaction with light. Here, we show that the role of the delocalized modes ($\xi(\Lambda) \geq L$) is more subtle. In the limit of large systems $L \to \infty$ the measure of those states in the spectrum rapidly falls as $\mu \sim \mathrm{e}^{-L/\gamma} \ln(L)$, where we have assumed logarithmic singularities for both $\xi(\Lambda)$ and $\varrho(\Lambda)$, with $\alpha = \gamma$. However, despite the zero measure of the delocalized states, they still affect the optical properties of the composite as shown below.

Relying on the scaling properties of the SP eigenproblem, we develop a scaling theory for the ensemble-averaged high-order moments

$$M_{n,m} = \left\langle S^{-1} \int |\boldsymbol{E}(\boldsymbol{r})/\boldsymbol{E}_0|^n [\boldsymbol{E}(\boldsymbol{r})/\boldsymbol{E}_0]^m \,\mathrm{d}\boldsymbol{r} \right\rangle \tag{3}$$

of the local electric fields $\boldsymbol{E}(\boldsymbol{r}) = -\nabla\varphi(\boldsymbol{r})$, where the integration is over the film surface S. We follow the approach developed in [25] and expand the local potential $\varphi(\boldsymbol{r}) = \int a(\Lambda)\Psi_n(\Lambda, \boldsymbol{r}) \,\mathrm{d}\boldsymbol{r}$ over the SP eigenstates. In zero approximation (in terms of κ), the weight coefficient $a^{(0)}(\Lambda) = \Pi_{\boldsymbol{E}_0}(\Lambda)/(\Lambda + \mathrm{i}\kappa)$ depends on the projection $\Pi_{\boldsymbol{E}_0}(\Lambda) = \int \Psi(\Lambda, \boldsymbol{r})[\boldsymbol{E}_0 \cdot \nabla\varepsilon(\boldsymbol{r})] \,\mathrm{d}\boldsymbol{r}$ of the external field $\boldsymbol{E}_0$ on the eigenstates. Assuming exponential localization of the SP eigenmodes with localization length $\xi(\Lambda)$, it is possible to obtain a simple scaling relationship for the high-order local field moments of the form

$$M_{n,m} \simeq \int \frac{\varrho(\Lambda)[a/\xi(\Lambda)]^{2(n+m-1)}}{[\Lambda^2 + \kappa^2]^{(n+m)/2}} \,\mathrm{e}^{\mathrm{i}m\phi(\kappa,\Lambda)} \,\mathrm{d}\Lambda \simeq \kappa^{-\varkappa_{n,m}} , \tag{4}$$

where $\varkappa_{n,m} = (n+m-1)(1-2\gamma) + \gamma$ is a positive scaling exponent ($n \geq 1$), κ is the loss factor and $\phi(\kappa, \Lambda) = \tan^{-1}(\kappa/\Lambda)$ in a phase factor.

In the derivation of (4) we use $\alpha = \gamma$, which agrees with our numerical results. Note that the singularity's critical index γ affects the high-order field moments through its contribution to the index $\varkappa_{n,m}$. The previously reported result [2], which was obtained based on the assumption that all modes are localized, can be retrieved from the formula above by setting $\gamma = 0$. Thus, (4) corrects the former theory [2] by taking into account the delocalized states.

It is possible to recover (4) by considering the local field as a set of peaks with characteristic size $l_p^* \simeq \xi(\kappa)$, magnitude $E_m^* \sim E_0 \kappa^{-1+2\gamma}$ and separation distance between them proportional to $\xi_e^* \sim l_p^* \kappa^{(-1+3\gamma)/2}$. Based on this similarity, the theory can be extended to frequencies that are away from the single-particle resonance ($\varepsilon'_{\rm m} = -\varepsilon_{\rm d}$). This is accomplished through renormalization of the system by dividing into segments with size $l_{\rm r} = a(|\varepsilon'_{\rm m}|/\varepsilon_{\rm d})^{\nu/(t+s)}$, where t, s and ν are the critical exponents for the static conductivity, dielectric constant and percolation correlation length, respectively. At the new length scale, the effective dielectric constants of the segments $\varepsilon_{\rm m}(l_{\rm r})$ and $\varepsilon_{\rm d}(l_{\rm r})$ possess the same resonance properties $\varepsilon_{\rm m}(l_{\rm r})/\varepsilon_{\rm d}(l_{\rm r}) \simeq -1 + {\rm i}\kappa$ as the original SP eigenproblem. Taking into consideration that the electric field is renormalized as $E_m \sim (l_{\rm r}/a)E_m^*$ and the new field separation length is $\xi_e \sim (l_{\rm r}/a)\xi_e^*$, the field moments are estimated as

$$M_{n,m} \simeq \left(\frac{|\varepsilon'_{\rm m}|}{\varepsilon''_{\rm m}}\right)^{\varkappa_{n,m}} \left(\frac{|\varepsilon'_{\rm m}|}{\varepsilon_{\rm d}}\right)^{\frac{\nu(n+m-2)+s}{s+t}}, \qquad (5)$$

where we have used the scaling relationship $n(l_{\rm r}) \propto (l_{\rm r}/a)^{s/\nu}$ for the number of peaks in each segment. Note that, at the single-particle resonance $\varepsilon'_{\rm m} = -\varepsilon_{\rm d}$, (5) is reduced to the previous result (4).

To examine the frequency dependence of the moments $M_{n,m}$, we consider noble metals and use the Drude model for the dielectric constant $\varepsilon_{\rm m}(\omega) \simeq \varepsilon_{\rm b} - (\omega_{\rm p}/\omega)^2/(1 + {\rm i}\omega_\tau/\omega)$, where $\varepsilon_{\rm b}$ is the interband transition term, $\omega_{\rm p}$ is the plasma frequency and $\omega_\tau \ll \omega_{\rm p}$ is the relaxation rate [26]. Applying the exact block elimination method [6], we check (5) for Ag composites in the high-frequency range $\omega_{\rm p} > \omega > \omega_\tau$. The results are shown in Fig. 3. Clearly, there is an excellent correlation between the numerical simulations and theoretical results. In both cases the field moments gradually decrease with the increase of the frequency and converge toward unity for $\omega = \omega_{\rm p}/\sqrt{\varepsilon_{\rm b}}$.

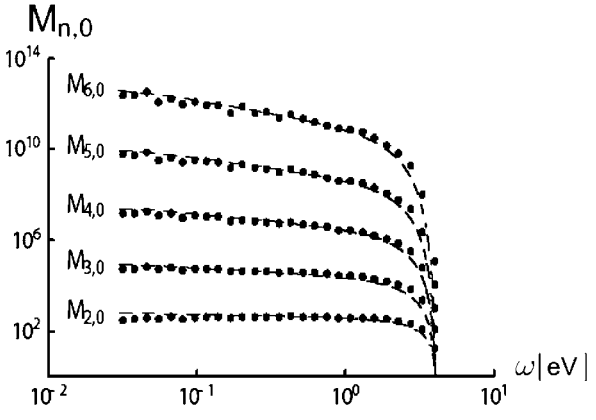

FIGURE 3 The local field moments $M_{n,0}$ (*dots*) are calculated with the exact numerical method and compared to the analytical results with exponent $\gamma = 0.14$ (*dashed lines*). The numerical data is averaged over 20 realizations of percolation systems with size $L = 250$. In the analytical estimates we use $t \simeq s \simeq \nu \simeq 4/3$ [1]

The local field enhancement, manifested through the high-order field moments, is directly measured in various linear and nonlinear optical processes. For example, surface-enhanced Raman scattering has been shown to be proportional to $M_{4,0}$, while the enhancement of Kerr optical nonlinearity is given by $M_{2,2}$ [1, 2, 27]. Thus, experimental investigation of these processes and their spectral dependences can result in further insight into the localization properties of the SP eigenmodes.

3 Experiment

To experimentally test the existence of delocalized states, we probed the delocalization exponent for the high-order moments of local intensity. Using a near-field scanning optical microscope (NSOM), we measured the near-field intensity distribution across semicontinuous silver films at the percolation threshold, and obtained the high-order moments of near-field intensities.

The semicontinuous silver films on glass substrates were synthesized by pulsed laser deposition [18]. Transmission electron microscope (TEM) images show that the samples are composed of individual silver grains with an average size of 10–15 nm. An increase in deposition time (surface concentration of silver) induces a structural transition from isolated metal grains ($p \leq 0.4$) to interconnected metal clusters ($p \approx 0.6$) and finally to a nearly continuous metal film with dielectric voids ($p \geq 0.8$). For these samples, the percolation threshold was found to be at $p_{\rm c} \approx 0.65$ [18]. In the near-field experiment, the samples were illuminated by the evanescent field (in total internal reflection geometry) of He-Ne lasers operating at 543 nm and 633 nm (p-polarized). The local optical signal was collected by a tapered, uncoated optical fiber with a tip radius ~ 50 nm. The tip-to-sample distance, controlled by shear-force feedback, was about 10 nm. The tip resolution was estimated at ~ 150 nm from the smallest features present in the near-field images [18]. The near-field intensity distribution was measured over several samples at the percolation threshold.

In Fig. 4 we present NSOM images showing the intensity distribution over a 8×8 μm area of a percolating silver film at two wavelengths 543 nm (Fig. 4a) and 633 nm (Fig. 4d). The intensity distribution across the sample is inhomogeneous, with hot spots of various sizes and amplitudes. The locations of the field maxima are very sensitive to wavelength, and the NSOM image changes completely upon a change of probe wavelength. Numerical calculations were also performed at $\lambda = 543$ nm (Fig. 4c) and 633 nm (Fig. 4f). A comparison of the NSOM images to the numerically calculated intensity distributions reveals that the minimum feature size in the measured intensity distribution corresponds to the resolution limit of the NSOM tip (~ 150 nm), whereas the smallest feature size in the numerical data is of the order of the grain size (~ 10 nm). Consequently, the local field enhancement factors are significantly lower in the experimental data. The numerical data were averaged over an area corresponding to the resolution limit of the NSOM. The resulting images,

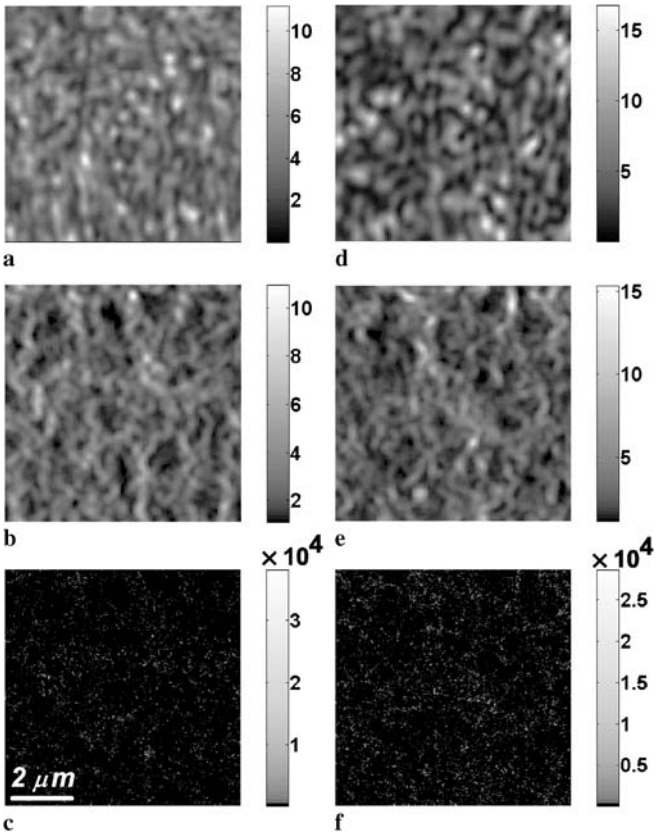

FIGURE 4 Local intensity distribution over a $8 \times 8\,\mu$m area of a semicontinuous silver–glass film at the percolation threshold at illumination wavelengths 543 nm (**a**, **b**, **c**) and 633 nm (**d**, **e**, **f**). (**a**) and (**d**) are obtained from NSOM measurements. (**c**) and (**f**) are numerically calculated intensity distributions. (**b**) and (**e**) are numerically calculations with spatial averaging to account for the NSOM tip resolution. The *scale bar* gives the intensity enhancement factor

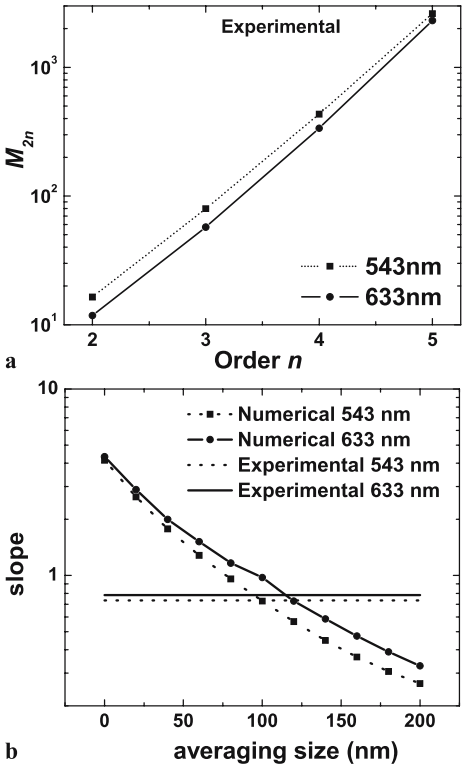

FIGURE 5 (**a**) Log–linear plot of the measured near-field intensity moments M_{2n} versus the order n at $\lambda = 543$ nm (*squares*) and 633 nm (*circles*). (**b**) The slope of $\log(M_{2n})$ over n obtained from the averaged numerical data as a function of the averaging size d. The experimental values of the slopes are marked by the *horizontal lines*

shown in Fig. 4b and e, are similar to the experimental images in terms of both feature size and local field enhancement factors.

From the NSOM images, we calculated the local intensity moments $M_{2n} = \langle I(x, y)^n \rangle / I_0^n$, where $I(x, y)$ is the near-field intensity and I_0 is the constant intensity of the incident light. Figure 5a is a log–linear plot of M_{2n} versus n for both wavelengths. $\log(M_{2n})$ increases almost linearly with n, as theoretically predicted in (4). However, the slopes of the experimental curves are considerably lower than the theoretical values. This reduction, as well as the reduction in the values of M_{2n}, is caused by the spatial averaging of the NSOM tip. To account for this effect, the numerical data are averaged over a square of dimension d situated 10 nm above the substrate. Figure 5b shows that the slopes decrease as the averaging size d increases. When the slopes are reduced to the experimental values (marked by the horizontal lines), the averaging size is consistent with our NSOM resolution. Additional confirmation for this averaging size comes from the agreement between the calculated intensity variance at this averaging size and the experimental values of variance. These agreements provide experimental validation of the numerical calculation, which gives the critical exponent without tip averaging $\gamma \approx 0.1$ at both wavelengths 543 nm and 633 nm. This value is close to the value of 0.14 obtained in Sect. 2, and confirms a tangible presence of delocalized SP modes.

4 Conclusion

In summary, we have investigated surface plasmon (SP) excitation in random metal–dielectric films. The Kirchhoff Hamiltonian (KH) describing the system exhibits unique short-range correlations between the diagonal and off-diagonal elements. These correlations, occurring because of local current conservation, result in a localization–delocalization transition for the electromagnetic response of the composite. This transition is manifested as a singularity in the center of the spectrum and corresponds to a zero-measure subset of delocalized SP eigenstates. This type of delocalization is inherent only in the correlated KH and is not present in the non-correlated discrete Anderson analogue. The scaling theory that is developed accounts for both localized and delocalized SP eigenmodes and describes the high-order field moments responsible for the nonlinear optical response of the system. Despite the zero measure of SP delocalization, it is found that it still affects the optical properties of the composite by modifying the critical indices in the field moments. Such a modification is confirmed experimentally by the near-field measurement of high-order intensity moments for percolating silver films on glass substrates. A good agreement between the experimental data and the numerical simulation results reveals the existence of delocalized SP states in semicontinuous silver films at the percolation threshold.

ACKNOWLEDGEMENTS This work was supported in part by NSF grants ECS-0210445, HRD-0317722, DMR-0093949, and DMR-007097 by NASA grant NCC-1035 and by ARO grant DAAD19-01-1-0682.

REFERENCES

1 V.M. Shalaev, *Nonlinear Optics of Random Media* (Springer, Berlin, 2000)
2 A.K. Sarychev, V.M. Shalaev, Phys. Rep. **335**, 275 (2000)
3 M.I. Stockman, S.V. Faleev, D.J. Bergman, Phys. Rev. Lett. **87**, 167 401 (2001)
4 M.I. Stockman, T.F. George, V.M. Shalaev, Phys. Rev. B **44**, 115 (1991)
5 M.I. Stockman, Phys. Rev. E **56**, 6494 (1997)
6 D.A. Genov, A.K. Sarychev, V.M. Shalaev, Phys. Rev. E **67**, 056 611 (2003)
7 D.A. Genov, A.K. Sarychev, V.M. Shalaev, Phys. Rev. B **72**, 113 102 (2005)
8 A.K. Sarychev, V.A. Shubin, V.M. Shalaev, Phys. Rev. B **60**, 16 389 (1999)
9 A.K. Sarychev, D.J. Bergman, Y. Yagil, Phys. Rev. B **51**, 5366 (1995)
10 J.A. Sanchez-Gil, J.V. Garcia-Ramos, E. Mendez, Phys. Rev. B **62**, 10 515 (2000)
11 L. Zekri, R. Bouamrane, N. Zekri, F. Brouers, J. Phys.: Condens. Matter **12**, 283 (2000)
12 S.I. Bozhevolnyi, V.S. Volkov, K. Leosson, Phys. Rev. Lett. **89**, 186 801 (2002)
13 S.I. Bozhevolnyi, Phys. Rev. Lett. **90**, 197 403 (2003)
14 D.P. Tsai, J. Kovacs, Z. Wang, M. Moskovits, V.M. Shalaev, J. Suh, R. Botet, Phys. Rev. Lett. **72**, 4149 (1994)
15 S.I. Bozhevolnyi, V.A. Markel, V. Coello, W. Kim, V.M. Shalaev, Phys. Rev. B **58**, 11 441 (1998)
16 S. Gresillon, L. Aigouy, A.C. Boccara, J.C. Rivoal, X. Quelin, C. Desmarest, P. Gadenne, V.A. Shubin, A.K. Sarychev, V.M. Shalaev, Phys. Rev. Lett. **82**, 4520 (1999)
17 S. Ducourtieux, V.A. Podolskiy, S. Gresillon, S. Buil, P. Gadenne, A.C. Boccara, J.C. Rivoal, W.A. Bragg, K. Banerjee, V.P. Safonov, V.P. Drachev, Z.C. Ying, A.K. Sarychev, V.M. Shalaev, Phys. Rev. B **64**, 165 403 (2001)
18 K. Seal, M.A. Nelson, Z.C. Ying, D.A. Genov, A.K. Sarychev, V.M. Shalaev, Phys. Rev. B **67**, 35 318 (2003)
19 K. Seal, M.A. Nelson, Z.C. Ying, D.A. Genov, A.K. Sarychev, V.M. Shalaev, Phys. Rev. B **94**, 226 101 (2005)
20 S.I. Bozhevolnyi, V. Coello, Phys. Rev. B **64**, 115 414 (2001)
21 P.W. Anderson, Phys. Rev. **109**, 1492 (1958)
22 I.M. Lifshits, S.A. Gredeskul, L.A. Pastur, *Introduction to the Theory of Disordered Systems* (Wiley, New York, 1988)
23 B. Kramer, A. MacKinnon, Rep. Prog. Phys. **56**, 1469 (1993)
24 D.J. Bergman, D. Stroud, Solid State Phys. **46**, 147 (1992)
25 D.A. Genov, A.K. Sarychev, V.M. Shalaev, A. Wei, Nano Lett. **4**, 153 (2004)
26 E.D. Palik (ed.), *Handbook of Optical Constants of Solids* (Academic, New York, 1985)
27 M. Moskovits, Rev. Mod. Phys. **57**, 783 (1985)